Food Science of Animal Products

Research Article

Effect of cold chain interruption on the metabolic composition and quality properties of fresh beef

Zhanfei Deng, Shuangshuang Sun, Yuyue Shi, Yayun Hu, Xin Lü, Yuanyuan Shan ✉

College of Food Science and Engineering, Northwest A&F University, Yangling 712000, China

✉Address correspondence to Yuanyuan Shan, shanyuanyuan@nwafu.edu.cn

Received: February 28, 2024; Revised: May 5, 2024; Accepted: May 23, 2024

Abstract: Cold chain disruption during logistics is a critical cause of food quality degradation. This study simulated 3 possible cold chain patterns and combined liquid chromatography-mass spectrometry (LC-MS) and gas chromatography-MS (GC-MS) to explore the quality deterioration and metabolic changes of fresh beef under cold chain disruption. The findings revealed that the cold chain interruption led to an upregulation of metabolites associated with lipid metabolism and protein degradation, which are linked to severe quality deterioration. Specifically, *L*-valine, *L*-isoleucine, *β*-alanine, 12-ketoeicosatetraenoic acid, and 5,6-epoxyeicosatrienoic acid exhibited upregulation. Tricarboxylic acid cycle intermediate metabolites oxoglutaric acid is a pivotal up-regulated metabolite that links protein degradation processes and post-slaughter energy production. Additionally, carbonyl compounds showed significant alterations in the beef under cold chain disruptions. Moreover, the later stage of cold chain disruption triggered a rapid collapse of beef quality. This study combined GC-MS and LC-MS to identify key metabolites associated with quality deterioration caused by cold chain disruption, providing a new perspective on beef quality monitor in cold logistics circulation.

Keywords: cold chain interruption; liquid chromatography-mass spectrometry; gas chromatography-mass spectrometry; beef quality; oxoglutaric acid

Citation: Z. F. Deng, S. S. Sun, Y. Y. Shi, et al., Effect of cold chain interruption on the metabolic composition and quality properties of fresh beef, Food Sci. Anim. Prod. 2 (2024) 9240060. https://doi.org/10.26599/FSAP.2023.9240060.

1 Introduction

Beef is highly nutritious, being low in fat and rich in essential proteins, vitamins, and minerals[1]. Beef carcass production was up to 67.88 million metric tons in 2020[2]. The abundant nutrients in meat provide an optimal environment that fosters microbial growth, thus resulting in meat spoilage and foodborne diseases. Microbial reproduction, protein degradation, and fat oxidation are the leading causes of beef spoilage. Unstable and unsuitable storage temperatures can accelerate the spoilage of beef[3–5]. Therefore, to meet consumers' demand for maintaining meat product quality and safety, extending shelf life, and reducing the risk of foodborne diseases, cold chain has become an important topic[6].

Cold chain logistics are extensively utilized in the transportation of meat after slaughter and its subsequent retail process to suppress microbial growth and lipid oxidation, thereby prolonging the meat's shelf life. Temperature control during cold chain logistics has been considered one of the most influential factors affecting chilled food quality[7]. Lorentzen et al.[8] proved that minor temperature variations in the commercial cold chain cause the deterioration of the cod fillets' quality and the reduction of shelf life. Tang et al.[9] investigated the impact of temperature fluctuation during the storage and transportation processes on the quality of tuna. They set up a cold chain condition with repeated alternation between −55 °C for storage and −18 °C for transportation. The results indicated that frequent temperature shifts in the cold chain significantly reduced the water-holding capacity and hardness of the tuna, and limited its retail value. Moreover, this effect became more pronounced with an increase in the frequency of temperature shifts. Yu et al.[10] also proved that cold chain interruption accelerated the loss of polyunsaturated fatty acids and the increase of unpleasant odors in salmon. In a previous study, the negative impact of temperature variation on beef quality during frozen storage was elucidated, with an increase in temperature variation, the rate of thaw loss and total volatile essential nitrogen value increased[3]. These studies indicate that the deterioration of fresh meat quality caused by temperature changes in cold chain logistics can further lead to food waste and economic losses.

However, in certain scenarios, factors such as the lack and uneven distribution of cold chain facilities, outdated low-temperature control technology during the cold chain process, the absence of a cold chain monitoring system, and the inevitable multiple handling of goods during circulation can all lead to the disruption of the cold chain. This disruption can, in turn, result in the deterioration of beef quality[11]. Accelerating the development of online monitoring for fresh meat quality during cold chain distribution is vital to safeguarding the quality and safety of these products[12], and identifying biomarkers of quality deterioration is key to establishing an effective monitoring system. Metabolomics, as a critical, high-throughput means of substance identification, can reveal the metabolite composition of substances, revealing the key metabolites and changes in biochemical reactions.

Thus, this study simulated 3 common cold chain interruption scenarios, conducted physicochemical property evaluation of beef under continuous and interrupted cold chain conditions, and utilized liquid chromatography-mass spectrometry (LC-MS) and gas chromatography-mass spectrometry (GC-MS) to identify

changes in beef metabolites during cold chain interruptions. Key metabolites associated with quality deterioration during cold chain breaks were identified by correlating physicochemical and metabolomic data. This study provides a new perspective for developing an online monitoring method for the quality of fresh beef in the cold chain, which is beneficial for ensuring the quality and safety of fresh meat products.

2 Materials and methods

2.1 Beef sample acquisition

Freshly slaughtered hot-deboning beef loin was purchased from a local abattoir, characterized by a red, shiny, non-sticky surface, and an elastic texture. Post-hot-deboning, the loin was immediately placed into a lidded foam box containing ice packs for temperature preservation. It was then transported to the laboratory within 1 h to maintain the initial freshness of the beef samples.

2.2 Sample handling

The loin was cut and grouped under 4 ℃ to ensure the preservation of the initial freshness of the beef samples for the simulated cold chain logistics experiment, with each piece having a size of 4 cm × 4 cm × 4 cm and a mass of 50 g; the quality assessment for fresh samples was immediately conducted, after which the samples were randomly divided into 4 groups. These groups were then packed into containers (6 cm × 6 cm × 6 cm) and maintained at 4 ℃. Then, simulated cold chain disruptions due to turnaround during transportation in 4 days to investigate the influence of cold chain disruption frequency on quality and metabolic changes of chilled beef. Four groups were labeled as C, L1, L2, and L3. Group C serves as the control group, representing the initial quality of fresh beef, and the beef sample in group C not subjected to any temperature variation treatments; group L1 maintained a cold chain at 4 ℃ throughout the process; group L2 involved transportation at 25 ℃ twice, on the 2nd and 4th day, respectively; group L3 involved transportation at 25 ℃ on the 3rd day. The duration of a single cold chain disruption is set to 12 h. On the day of the cold chain disruption, except for the period of the disruption, the remaining time is maintained at 4 ℃ (Table S1). On the 1st, 2nd, 3rd, 4th, and 5th day, samples in each group were taken out for quality assessment, and metabolomics analysis was conducted on the last day. Three replicates were performed for each experiment.

2.3 Quality evaluation

2.3.1 Appearance observation

Photographs were taken to observe changes in the appearance of the meat during the simulated cold chain process, and the meat used to take the photographs was fixed for each group. CS-820N Colorimeter (Hangzhou CHNSpec Technology Co., Ltd., China) was used to detect the color changes induced by cold chain disruption. The values of lightness (L^*), redness (a^*), and yellowness (b^*) were obtained after whiteboard and blackboard correction, and before color measurement, blooming was not performed.

2.3.2 Analysis of total volatile basic nitrogen (TVB-N) content

The micro diffusion method was applied[13]. The meat sample was cut, placed in a beaker, stirred with distilled water, and filtered. The filtrate was taken to determine the TVB-N content using the K9860 automated Nitrogen Analyzer (Hanon Advanced Technology Group Co., Ltd.). TVB-N content was calculated by equation (1):

$$\text{TVB-N content}\,(\text{mg}/100\ \text{g}) = \frac{(V_1 - V_2) \times c \times 14 \times 20}{m} \times 100 \quad (1)$$

Where V_1 represents the volume of hydrochloric acid standard solution consumed by the sample solution (mL); V_2 represents reagent blank consumed hydrochloric acid volume (mL); c represents the actual concentration of hydrochloric acid standard solution (mol/mL); m represents the mass of the sample (g).

2.3.3 Thiobarbituric acid reactive substances (TBARS) value analysis

TBARS value in meat were conducted using the spectrophotometric method, referring to the previous report[14]. Malondialdehyde (MDA) was extracted by trichloroacetic acid (TBA) solution and reacted with TBA to form a pink compound and detect its absorbance value at 532 nm wavelength by ultraviolet spectrophotometer (Shimadzu (China) Co., Ltd.), then compared with the standard series. TBARS value was calculated by equation (2):

$$\text{TBARS value}\,(\text{mg/kg}) = \rho \times \frac{V}{m_1} \quad (2)$$

Where ρ represents concentration of MDA in the sample solution obtained from the standard series curve (μg/mL); V represents volume of the sample solution (mL); m_1 represents mass of the final sample solution (g).

2.3.4 Drip loss analysis

Beef samples were persevered in a flat plate. Weight the mass of the absorbent paper and the use absorbent paper to absorb the water from the surface of the beef sample and in the dish, then evaluate the mass of the absorbent paper[15]. The drip loss was calculated by equation (3):

$$\text{Drip loss}\ (\%) = \frac{m_2 - m_0}{m} \times 100 \quad (3)$$

Where m represents the premier mass of the sample (g); m_2 represents mass of the absorbent paper after absorption (g); m_0 represents mass of the absorbent paper before absorption (g).

2.3.5 Shear force analysis

The beef was steamed at high temperature before shear force measurement. Shear force values were recorded using a texture analyzer (TA.XT Plus, Stable Micro Systems, Surrey, UK) with HDP/BS blade. The pre-test and post-test speeds were 2 and 10 mm/s, respectively. The test speed was 1 mm/s with a distance of 25 mm[16]. The maximum force to cut into the sample was recorded as the shear force.

2.3.6 Total viable count (TVC) analysis

Sampling for the determination of the TVC was conducted daily from day 1 to day 5. Microbial analyses were performed using the total colony count method[17]. The procedure entailed the following steps: 1 g sample was minced with sterile scissors, after which 10 mL of 0.9 g/100 mL saline solution was added. The mixture was then homogenized in a sterile bag to form a homogenate. Then, the obtained solution was diluted 1 000 times, and 200 μL was spread onto the LP agar medium. The medium was incubated at a temperature of 37 ℃ for a period of 36 to 48 h, following which the colonies were enumerated.

2.4 LC-MS and GC-MS analysis

The analysis of the metabolite profiling was conducted by Suzhou PANOMIX Biomedical Tech Co., Ltd. The samples were collected on the 5th day of the cold chain process. Approximately 400 mg of beef was taken under conditions of 4 °C, wrapped in tin foil, flash-frozen in liquid nitrogen, and then transported in a dry ice box to Panomics Inc. for subsequent analysis. The raw data were processed using R XCMS (v3.12.0) for feature detection[18], retention time correction, and alignment. The batch effect was then eliminated by correcting the data based on quality control (QC) samples. Metabolites with relative standard deviation (RSD) greater than 30% in QC samples were filtered and used for subsequent data analysis. The metabolites were identified by accuracy mass and secondary mass spectrometry (MS/MS) data, which were matched with Human Metabolome Database[19], Kyoto Encyclopedia of Genes and Genomes (KEGG)[20], Lipid Maps[21], and the metabolite database built by PANOMIX Biomedical Tech Co., Ltd., (Suzhou, China). The molecular formula was predicted by adduct ion, then matched with the database to realize MS identification of metabolites. At the same time, the MS/MS data from the quantitative table were compared with the fragment ions and other information about each metabolite in the database to realize the MS/MS identification of metabolites.

2.5 Statistical analysis

A one-way ANOVA was performed to illuminate the data at IBM SPSS Statistics 20.0 (SPSS Inc., Chicago, Illinois, USA); Duncan's test was employed to determine differences (significance was defined at $P < 0.05$). Principal component analysis (PCA), partial least squares discriminant analysis (PLS-DA), and orthogonal partial least squares discriminant analysis (OPLS-DA) were applied for metabolomics data analysis to discriminate the groups by R ropls (v1.22.0) package. By default, when $P < 0.05$ and variable importance in projection (VIP) > 1, metabolites were considered to have significant differential expression. MetaboAnalyst[22] subjected differential metabolites (DMs) to pathway analysis, identifying metabolites in metabolomics and then mapping to the KEGG pathway for biological interpretation of higher-level systemic functions. The metabolites and corresponding pathways were visualized using the KEGG Mapper tool. The outcomes were displayed as mean ± standard error (SE).

3 Results

3.1 Physicochemical properties

3.1.1 Appearance of beef samples during cold storage

Images of appearance were captured from day 1 to day 5. Group L1 maintained a temperature of 4 °C, and there were no obviously browning (Figure 1A), and no statistical difference in L^* and a^* during 5 days (Table S2). Conversely, groups L2 and L3 exhibited evident browning. The L^*, a^*, and b^* significantly decreased on the 5th day compared to the 1st day ($P < 0.05$; Table S2), suggesting that a stable cold chain at low temperatures is essential for maintaining the color of meat. In contrast, interruptions in the cold chain can result in significant browning.

3.1.2 TVB-N content change of beef during cold storage

TVB-N content is commonly used as a protein and amine degradation biomarker. At stable low temperatures, TVB-N contents were consistently stable in group L1, and continued to increase in both group L2 and L3 after a cold-chain interruption; for group L2, TVB-N contents continued to grow despite the reconnection of the cold chain, with the most significant increase occurring on the 4th to 5th day (Figure 1B). At the sales endpoint, the TVB-N contents of groups L1, L2, and L3 were 5.70, 32.85, and 18.79 mg/100 g, respectively.

3.1.3 TBARS value change of beef during cold storage

TBARS value was used to measure the effect of cold chain interruption on lipid peroxidation in beef. During the simulation, the TBARS value of group L1 was consistently low, and the TBARS value of group L3 increased after the cold chain interruption, still, it was not significantly different from group L1. The TBARS value of group L2 increased dramatically after the first cold chain interruption and was obviously higher than groups L1 and L3 (Figure 1C).

3.1.4 Drip loss change of beef during cold storage

Drip loss was used to evaluate the water retention capacity of the meat, and the interruption of the cold chain caused a sharp increase in drip loss of beef. In contrast, the reconnection of cold chain mitigated the drip loss increase. Compared to groups L2 and L3, the drip loss of group L1 was more stable in the first 4 days and elevated only on the 5th day (Figure 1D).

3.1.5 Shear force change of beef during cold storage

Shear force characterizes the tenderness and chewiness of meat. The shear force of beef after steaming during storage was determined, and the results showed that shear force tapered in all groups during storage, but cold chain disruption exacerbates this trend (Figure 1E).

3.1.6 TVC change of beef during cold storage

A total number of colonies is an essential indicator of meat freshness; the multiplication of microorganisms relies on temperature, and increasing temperature leads to mass reproduction. On day 4, the total number of bacterial colonies in groups L2 and L3 exceeded 6 (lg (CFU)/g) (Figure 1F), which is considered an upper limit of fresh meat[23].

3.2 Untargeted metabolomics analysis

3.2.1 Analysis overview

Raw MS data were processed for peak detection, peak filtering, and peak alignment, and the data were well quality-controlled based on QC samples, retaining substances with a coefficient of variation of less than 30% for subsequent analysis (Figure S1). In primary MS, 16 913 and 8 150 metabolites were characterized in the positive and negative ion mode, respectively, and MS/MS identified the class and formula of 468 metabolites. Classification results indicated that the top 10 categories that involved most DMs were carboxylic acids and derivatives, fatty acyls, organooxygen compounds, steroids and steroid derivatives, hydroxy acids and derivatives, organonitrogen compounds, indoles and derivatives, keto acids and derivatives, pyrimidine nucleosides, and benzene and substituted derivatives (Figure 2A).

3.2.2 Multivariate statistical analysis result

VIP scores derived from PLS-DA and P value were used to identify further the DMs between control and experiment groups. The DMs between the control and logistics groups were identified with the criteria of VIP > 1 and $P < 0.05$. We recognized the specific change of DMs by $\log_2$ fold change ($\log_2$FC); $\log_2$FC > 0 indicates

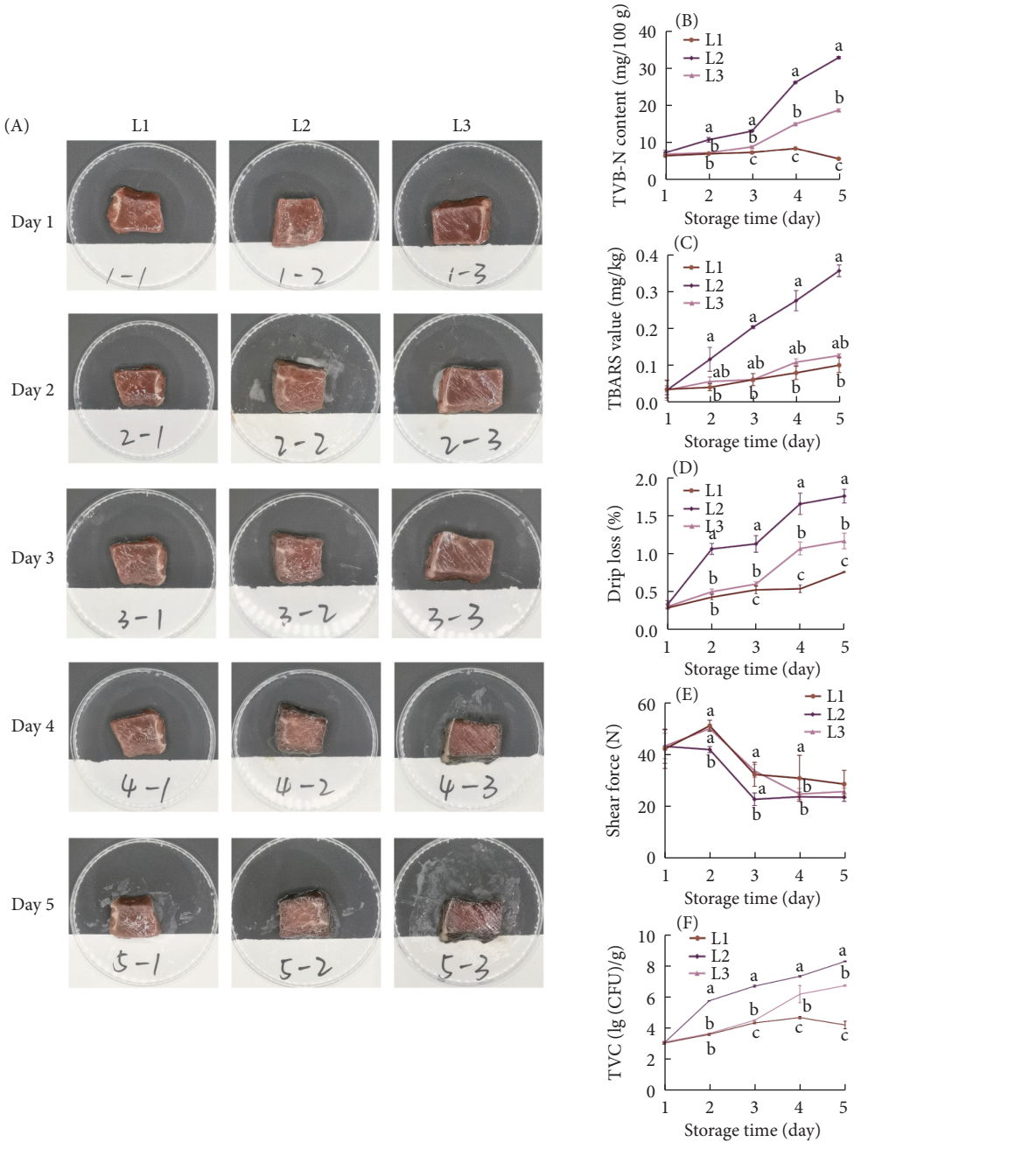

Figure 1 Effects of temperature fluctuations on fresh beef's appearance and physicochemical properties. (A) Appearance of logistics group beef on day 1 to day 5, (B) total volatile basic nitrogen (TVB-N) content, (C) thiobarbituric acid reactive substances (TBARS) value, (D) drip loss, (E) shear force, and (F) total viable count (TVC) changes during beef storage. The results are expressed as the mean ± standard error (n = 3). Different lowercase letters (a–c) indicate significant difference among groups ($P < 0.05$).

up-regulate while $\log_2$FC < 0 indicates down-regulated. In all group comparisons, the most extensive variety of metabolites was changed in group L2, up to 177, with 93 metabolites up-regulated and 84 metabolites down-regulated, far more than the 102 metabolites in L1 vs. C (Figure 2B). The upset plot exhibits the similarity of DMs between groups for comparison (Figure 2C). There were fewer DMs in L1 vs. C compared to L2 and L3, indicating that storage under stable cold temperatures is beneficial to maintaining beef quality. DMs of L2 and L3 vs. C overlap far more than L1, up to 74. Heat maps visualized the variation of volatile or non-volatile metabolites in each group; the clustering result illustrated an apparent discrepancy among control and logistics groups (Figures 2D and 3A). The Venn plot shows the overlap of the differential violate metabolites between each logistics group and the control group, with group L1 and L2 overlapping the least, group L2 and L3 overlapping the most, and L2-exclusive DMs the most (Figure 3B). PCA score plots in both positive and negative ion modes demonstrate that the metabolic composition of different groups changed (Figures 2E, F and 3C). According to the variation of non-volatile metabolites, groups L2 and L3 were significantly different from groups L1 and C, and group L1 is partly consistent with groups L2 and L3, pointing out that cold storage maintains beef quality to a certain degree for some time. However, slight quality deterioration still happens (Figure 2D), groups L3 and L1 have a similar composition in volatile metabolite substances, and group L2 represents a significant difference compared with the rest

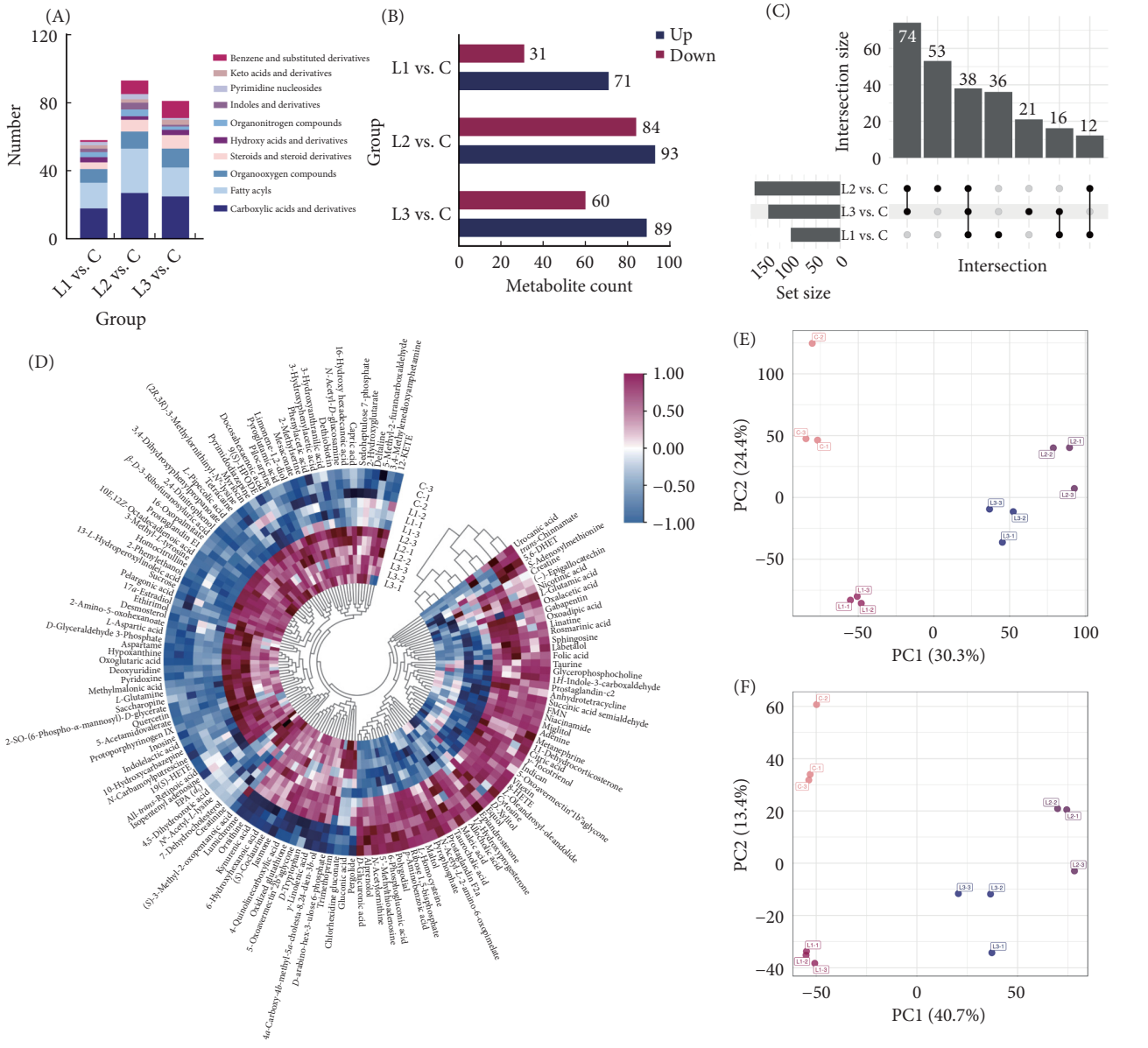

Figure 2 Liquid chromatography-mass spectrometry reveals metabolic changes in fresh beef under temperature fluctuations. (A) The top 10 categories with changed metabolites in the logistics group compared to the control; (B) Statistics on the number of up-regulated and down-regulated differential metabolites in the 3 logistic groups; (C) Upset plot of logistics group compared with control group; (D) Heatmap with cluster lines of all metabolites; (E and F) Principal component analysis (PCA) score plot in positive and negative ion mode, respectively. FMN, flavin mononucleotide; 5,6-DHET, 5,6-dihydroxy-eicosatetraenoic acid; 8-HETE, 8-hydroxy-5,6,10,12-eicosatetraenoic acid; 19(*S*)-HETE, 8,9,11,15-eicosatetraynoic acid.

of the groups (Figure 3A). The difference in volatile metabolites of groups L2 and L3 was more pronounced than the results of LC-MS, indicating that the prolonged time at 25 °C and more acute temperature variation contribute more to violate metabolite variation.

3.3 KEGG analysis result

DMs were characterized and involved in the KEGG pathway, and the network diagram associates statistically altered pathways and DMs in them, displaying the crucial metabolites that exist in several pathways simultaneously (Figure 4A). There are 13 pathways identically changed in groups L1, L2, and L3, in comparison to group C, 6 pathways changed only in L2 and L3, and 2 pathways only in L3 and L1. Groups L2 and L3 have the most overlapped pathways among the 3 logistics groups compared with group C, while groups L1 and L2 have the least. Except for the overlapped partition, groups L1, L2, and L3 have 4, 7, and 7 pathways that were individually altered relative to group C, respectively. Central carbon metabolism in cancer, arginine biosynthesis, alanine, aspartate and glutamate metabolism, ABC transporters, and lysine degradation were pathways involved in most DMs between logistics and control groups. Prostaglandin-c2, ornithine, oxoglutaric acid, 2-amino-5-oxohexanoate, *D*-ribose 5-phosphate, *N*-acetylornithine, *L*-valine, *L*-isoleucine and glyceric acid were DMs shared in 3 logistics groups, indicating that energy production, degradation of protein, and amino acids metabolism were the main metabolic change of beef under stable cold chain. Except the pathways overlapped with group L1, arachidonic acid metabolism, butanoate metabolism, glucagon signaling pathway, glutamatergic synapse, glyoxylate and dicarboxylate metabolism, and proximal tubule bicarbonate reclamation were significantly changed in both groups L2 and L3 (Figures 4B and C).

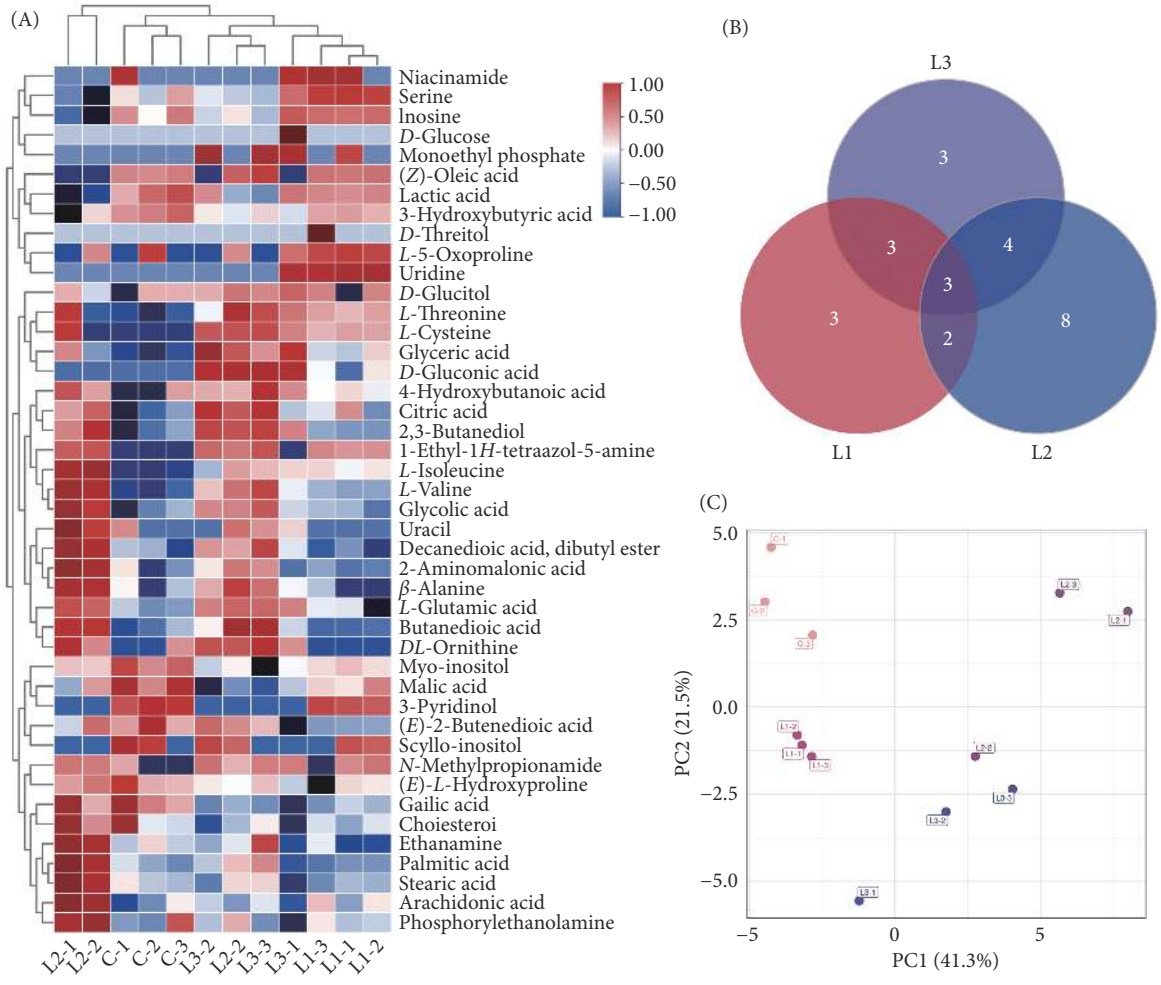

Figure 3 Gas chromatography-mass spectrometry detects metabolic changes between control and logistics groups. (A) Heatmap with cluster lines of all metabolites; (B) Venn plot of the overlapped and different metabolites in all groups; (C) PCA score plot.

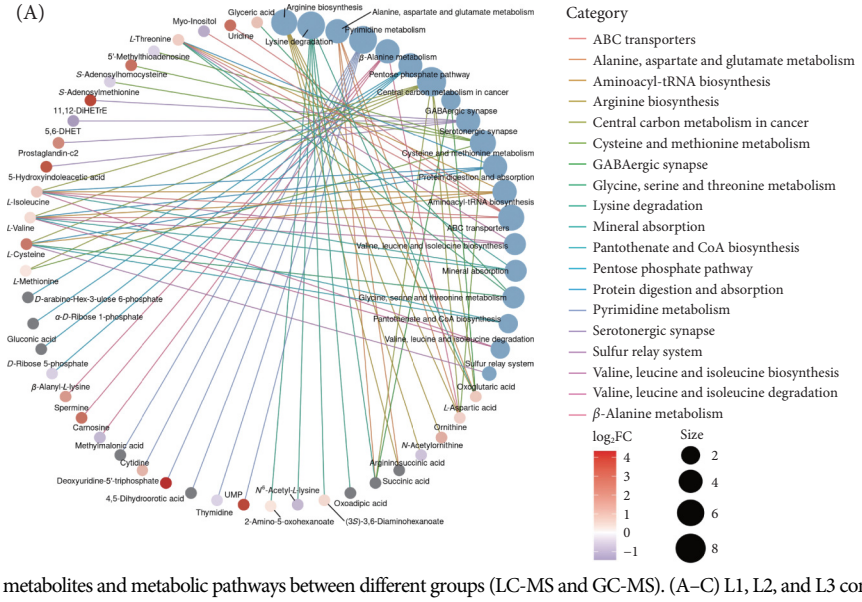

Figure 4 Significantly altered metabolites and metabolic pathways between different groups (LC-MS and GC-MS). (A–C) L1, L2, and L3 compared with C; (D) L2 and L3; (E and F) L2 and L3 compared to L1. Different color lines represent different pathways, and the positive and negative values of log_2FC indicate the up-regulation and down-regulation of metabolites, respectively. The size of the dot of paths shows the number of differential metabolites included. UMP, uridine monophosphate; IMP, inosine monophosphate; FMN, flavin mononucleotide; 16(*R*)-HETE, 15-hydroxy-5,8,11,13-eicosatetraenoic acid; 8-HETE, 8-hydroxy-5,6,10,12-eicosatetraenoic acid; 5,6-DHET, 5,6-dihydroxy-eicosatetraenoic acid; 19(*S*)-HETE, 8,9,11,15-eicosatetraynoic acid; 5-KETE, 5-keto-eicosatetraenoic acid; 3′-AMP, 3′-adenylic acid.

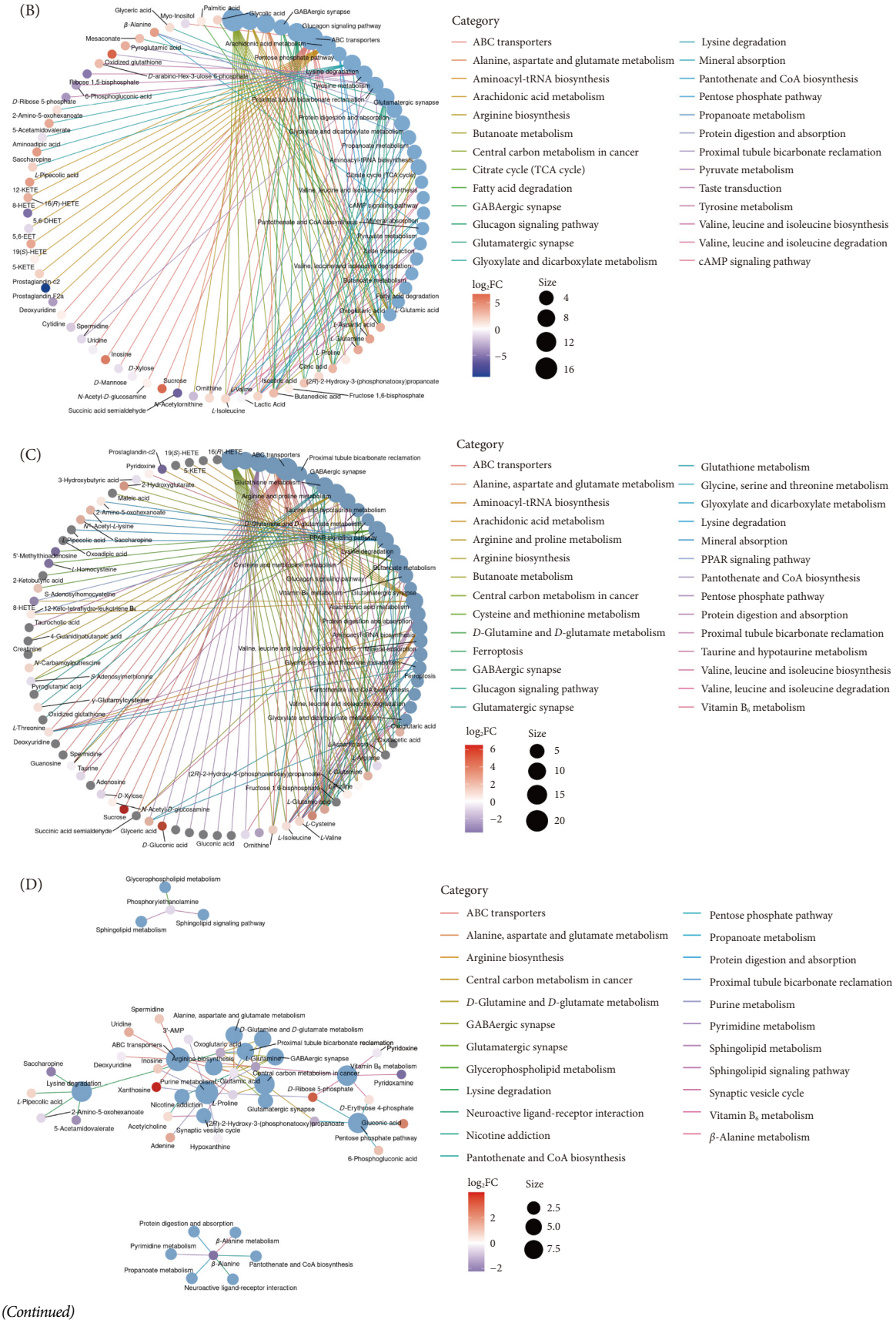

Figure 4 *(Continued)*

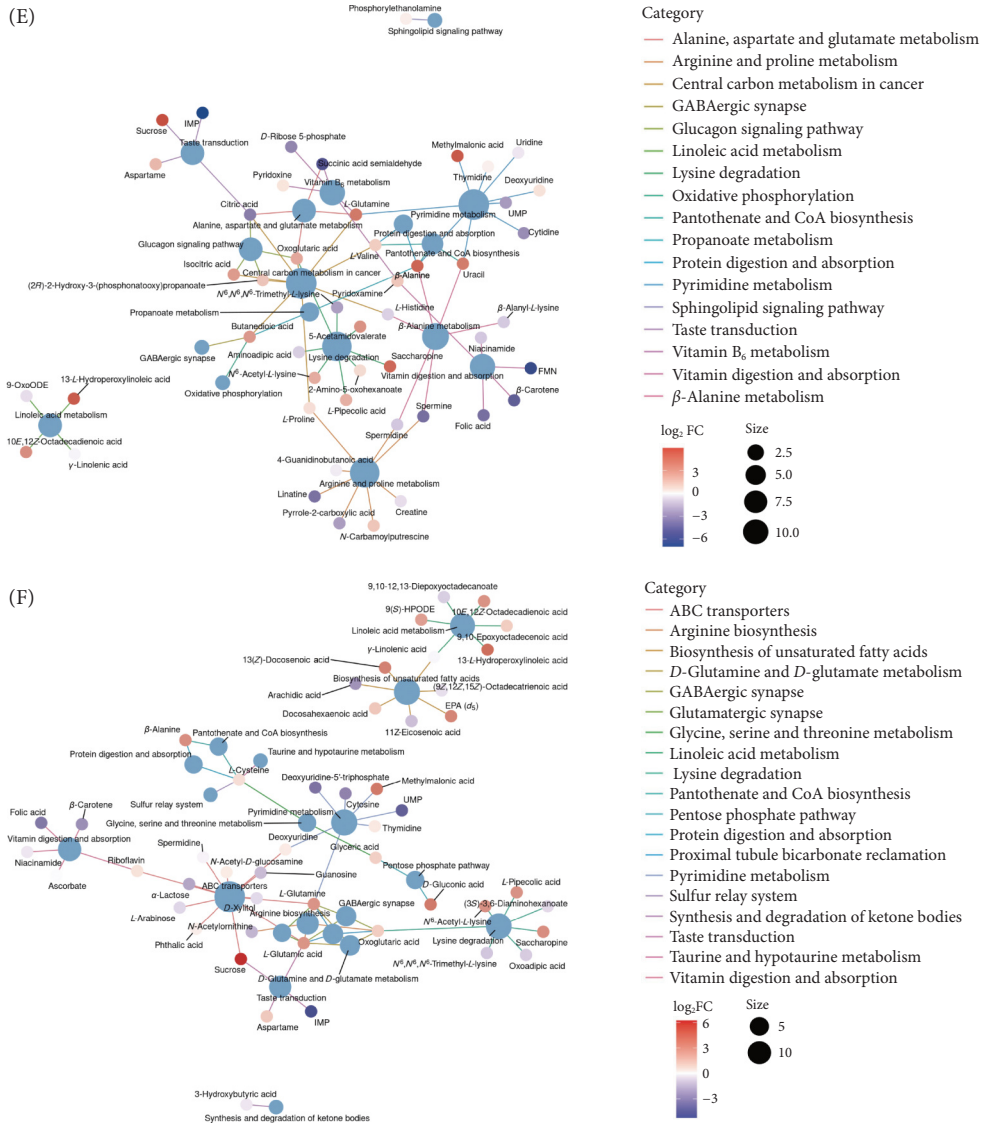

Figure 4 *(Continued)*

ABC transporters pathway showed that substances significantly regulated were transported by phosphate and amino acid transporters, mineral and organic ion transporters, oligosaccharide, polyol, lipid transporters, and monosaccharide transporters (Figure S2), and these materials mainly lie in amino acids, phosphates, lipids, and monosaccharides, which are accordance with the categories of DMs (Figure 2A). Arachidonate (AA) is a crucial metabolite in arachidonic acid metabolism, 12-ketoeicosatetraenoic acid (12-KETE), 15-hydroxy-5,8,11,13-eicosatetraenoic acid (16(*R*)-HETE), and 5,6-epoxyeicosatrienoic acid (5,6-EET) were up-regulated and directly metabolized from arachidonate (Figures 4B, C and S4). Compared with groups C and L1, lipid metabolites and amino acids like *L*-glutamic acid, oxoglutaric acid, glyceric acid, *L*-valine, 2-amino-5-oxohexanoate, and *L*-proline in groups L2 and L3 were up-regulated (Table 1), suggesting that cold chain disruption promote lipid and fatty acid metabolism and exacerbate the protein degradation. Glutathione metabolism, ABC transporters, and arachidonic acid metabolism are altered in groups L2 and L3 compared with L1 (Figures 4E and F). Compared with group L3, *L*-glutamic acid, oxoglutaric acid, and *L*-glutamine were upgraded in group L2 and linked multiple pathways (Figure 4D, Table 1). Alanine, aspartate and glutamate metabolism, arginine biosynthesis, *D*-glutamine and *D*-glutamate metabolism, and lysine degradation were the differential metabolic pathways of the groups L2 and L3 (Figure 4D).

3.4 Linkage of crucial metabolic pathways

To explore the correlation between DMs and differential pathways under cold chain disruption, we pick up the DMs that simultaneously appeared in several pathways and demonstrate the metabolic process in which they participate (Figure 5). In the overlapped partition, the tricarboxylic acid (TCA) cycle features an active metabolic pathway involving 3 DMs as its intermediate metabolites, accumulating oxoglutaric acid and isocitrate. Oxoglutaric acid is a pivotal metabolite that links many metabolic processes such as glutathione metabolism and alanine, aspartate, and glutamate metabolism; it also can transform into *L*-glutamate and glutathione, and further transformation into 5-oxoproline, oxidized glutathione, succinate semialdehyde, and *L*-glutamine. For the LC-MS results, arginine biosynthesis, alanine, aspartate and glutamate metabolism, linoleic acid metabolism, and arachidonic acid

Table 1 Differential metabolites that exist in significantly changed KEGG pathways among group L1, L2, and L3 compared to group C.

Metabolites	Precursor type	Group				*P* value	*m/z*	Retention time (s)
		C	L1	L2	L3			
(2*R*,3*R*)-3-Methylornithinyl-N^6-lysine	$[M+H]^+$	23.933 8 ± 0.654 3^{A}	24.216 4 ± 0.531 2^{A}	25.804 4 ± 0.247 4^{B}	25.473 1 ± 0.603 8^{B}	< 0.01	275.21	40.90
2-Amino-5-oxohexanoate	$[M+H]^+$	26.033 1 ± 0.119 8^{A}	26.362 9 ± 0.166 7^{B}	27.211 1 ± 0.110 0^{C}	26.654 2 ± 0.089 4^{D}	< 0.001	146.08	53.40
12-Hydroxyeicosatetraenoic acid	$[M+H]^+$	20.639 7 ± 0.150 9^{A}	22.156 3 ± 1.222 1^{A}	24.438 3 ± 0.844 0^{AB}	22.383 3 ± 1.643 1^{B}	< 0.05	319.22	520.20
16-Oxopalmitate	$[M+H]^+$	23.767 6 ± 0.317 9^{A}	22.855 6 ± 0.251 8^{A}	26.575 7 ± 0.812 5^{B}	27.059 1 ± 1.066 6^{B}	< 0.001	271.23	522.00
5,6-Dihydroxy-eicosatetraenoic Acid	$[M-H]^-$	22.126 9 ± 0.235 4^{A}	20.692 2 ± 0.202 4^{B}	20.903 6 ± 0.163 2^{B}	20.707 8 ± 0.189 5^{B}	< 0.001	337.24	464.70
5-Acetamidovalerate	$[M]^+$	22.978 5 ± 0.098 5^{A}	23.304 8 ± 0.445 4^{A}	26.401 9 ± 0.405 5^{B}	24.606 4 ± 0.925 0^{C}	< 0.001	159.09	178.20
8-Hydroxyeicosatetraenoic acid	$[M+H-H_2O]^+$	23.393 2 ± 0.294 6^{A}	23.104 3 ± 0.271 6^{A}	18.159 6 ± 0.440 1^{B}	20.009 7 ± 1.759 2^{C}	< 0.001	303.23	535.90
Allocholic acid	$[M]^+$	25.904 8 ± 0.402 6^{A}	26.378 4 ± 0.216 9^{A}	19.973 5 ± 2.609 5^{B}	21.114 8 ± 2.421 0^{B}	< 0.01	408.37	654.10
Alprenolol	$[M+H]^+$	30.929 2 ± 1.283 7^{A}	29.379 8 ± 0.453 9^{B}	25.842 8 ± 0.283 2^{C}	26.248 0 ± 0.296 8^{C}	< 0.001	250.18	411.70
Citrate	$[M-H]^-$	28.304 1 ± 1.211 9^{AB}	28.933 3 ± 0.096 4^{A}	25.483 2 ± 0.300 7^{B}	26.951 3 ± 0.916 9^{AB}	< 0.05	191.02	46.20
Creatine	$[M-H]^-$	28.246 9 ± 0.091 8^{A}	28.921 0 ± 0.080 3^{A}	28.319 1 ± 0.329 4^{A}	27.415 8 ± 0.705 5^{B}	< 0.05	130.06	51.60
Cytosine	$[M+H]^+$	22.081 6 ± 1.415 9^{A}	21.710 3 ± 0.897 9^{A}	20.267 4 ± 1.676 9^{AB}	18.872 8 ± 0.601 0^{B}	< 0.05	112.05	53.40
D-Arabino-hex-3-ulose 6-phosphate	$[M-H]^-$	19.739 1 ± 0.161 3^{A}	22.244 1 ± 0.093 0^{B}	22.205 8 ± 0.962 1^{B}	22.388 7 ± 0.576 9^{B}	< 0.01	259.02	69.70
Deoxyuridine	$[M]^+$	26.396 5 ± 0.008 1^{A}	26.421 5 ± 0.025 6^{A}	27.026 3 ± 0.093 4^{B}	26.755 5 ± 0.080 3^{C}	< 0.001	228.20	651.10
Docosahexaenoic acid	$[M-H]^-$	27.851 5 ± 0.286 3^{A}	27.329 9 ± 0.121 2^{A}	28.918 4 ± 0.355 8^{B}	28.537 9 ± 0.531 0^{B}	< 0.01	327.23	597.00
D-Tryptophan	$[M-H]^-$	24.324 3 ± 1.170 0^{A}	27.096 0 ± 0.136 5^{B}	26.511 3 ± 0.095 1^{B}	26.653 7 ± 0.076 6^{B}	< 0.01	203.08	127.00
D-Xylitol	$[M+H]^+$	20.587 8 ± 0.278 6^{AB}	20.853 8 ± 0.084 1^{A}	20.385 1 ± 0.195 9^{B}	20.253 2 ± 0.187 2^{B}	< 0.05	153.13	375.00
Eicosapentaenoic acid (d_5)	$[M]^-$	24.847 7 ± 0.118 6^{A}	24.069 9 ± 0.677 6^{A}	24.208 5 ± 0.378 3^{A}	27.387 5 ± 0.493 2^{B}	< 0.001	302.22	579.50
Ethirimol	$[M]^+$	21.659 5 ± 0.052 3^{A}	21.657 4 ± 0.137 3^{A}	24.060 0 ± 1.780 9^{B}	24.592 0 ± 0.453 8^{B}	< 0.01	209.15	479.00
Flavin mononucleotide	$[M-H]^-$	20.952 4 ± 0.201 3^{A}	20.791 8 ± 1.008 0^{A}	14.234 0 ± 0.997 5^{B}	18.356 6 ± 1.379 4^{C}	< 0.001	455.10	205.20
Folic acid	$[M]^-$	24.089 6 ± 0.237 5^{A}	25.208 1 ± 0.788 7^{B}	21.367 7 ± 0.612 8^{C}	22.087 6 ± 0.415 7^{C}	< 0.001	441.25	473.00
Gabapentin	$[M+H]^+$	24.624 6 ± 0.810 0^{A}	26.563 1 ± 0.072 1^{B}	23.764 8 ± 0.623 8^{A}	23.464 9 ± 0.723 4^{A}	< 0.01	172.13	289.30
γ-Linolenic acid	$[M]^-$	25.215 6 ± 0.074 5^{A}	26.505 7 ± 0.036 9^{B}	26.299 9 ± 0.035 6^{C}	26.384 9 ± 0.063 1^{C}	< 0.001	278.22	586.80
γ-Tocotrienol	$[M-H]^-$	20.800 2 ± 0.847 0^{A}	21.789 1 ± 0.960 1^{A}	17.279 1 ± 0.795 8^{B}	18.541 7 ± 1.480 4^{B}	< 0.01	409.31	548.20
Gluconic acid	$[M-H]^-$	25.278 6 ± 0.390 2^{A}	26.762 7 ± 0.133 9^{AB}	27.158 8 ± 1.581 2^{B}	29.878 6 ± 0.413 3^{C}	< 0.01	195.05	46.80
Indolelactic acid	$[M+H]^+$	23.932 6 ± 0.280 7^{AB}	23.684 3 ± 0.421 8^{A}	25.753 7 ± 0.334 0^{B}	24.781 7 ± 0.706 7^{C}	< 0.01	206.08	305.10
Inosine	$[M+H]^+$	27.375 9 ± 0.996 1^{A}	27.676 4 ± 0.436 6^{A}	32.922 7 ± 0.459 1^{B}	30.048 5 ± 1.714 8^{C}	< 0.001	269.09	65.10
Isocitric acid	$[M-H]^-$	28.213 1 ± 1.102 4^{A}	28.998 5 ± 0.144 7^{A}	29.215 7 ± 0.234 3^{B}	28.405 2 ± 1.237 2^{A}	< 0.05	191.02	40.40
Isopentenyl adenosine	$[M+H]^+$	18.827 3 ± 1.495 7^{AB}	17.689 7 ± 1.394 4^{A}	21.395 0 ± 0.341 5^{C}	20.429 0 ± 0.158 9^{BC}	< 0.05	336.16	291.40
Kynurenic acid	$[M+H]^+$	24.080 7 ± 0.154 6^{A}	25.169 6 ± 0.018 9^{B}	25.477 1 ± 0.266 4^{BC}	25.282 2 ± 0.031 6^{C}	< 0.001	190.05	213.60
Labetalol	$[M]^-$	21.954 6 ± 0.630 6^{A}	22.365 7 ± 0.413 9^{A}	19.882 3 ± 0.603 8^{B}	20.313 0 ± 0.131 2^{B}	< 0.001	328.18	465.70
L-Aspartic acid	$[M-H]^-$	22.268 5 ± 0.327 8^{A}	22.931 3 ± 0.225 7^{A}	25.839 3 ± 0.881 7^{B}	24.647 5 ± 1.110 3^{B}	< 0.01	132.03	46.30
L-Glutamic acid	$[M+H]^+$	24.949 5 ± 0.874 2^{A}	24.010 6 ± 1.041 6^{AB}	22.489 0 ± 0.385 2^{B}	20.132 8 ± 1.119 0^{C}	< 0.001	148.06	53.10
L-Glutamine	$[M+H]^+$	24.904 3 ± 0.176 1^{A}	23.984 8 ± 0.986 5^{A}	28.341 0 ± 0.159 8^{B}	26.890 4 ± 0.165 3^{C}	< 0.001	147.08	53.20
L-Homocysteine	$[M+H]^+$	25.930 8 ± 0.584 8^{A}	26.101 6 ± 0.115 3^{A}	22.405 1 ± 0.191 9^{B}	22.660 3 ± 0.073 0^{B}	< 0.001	136.05	689.60
Limonene-1,2-diol	$[M+H]^+$	20.030 4 ± 1.040 8^{A}	22.282 3 ± 1.044 2^{B}	25.417 4 ± 0.832 1^{BC}	23.779 4 ± 1.327 4^{C}	< 0.01	171.15	343.10
Linatine	$[M]^+$	22.945 6 ± 1.122 4^{A}	24.457 3 ± 0.166 7^{A}	20.223 0 ± 1.279 1^{B}	21.153 1 ± 0.407 6^{B}	< 0.01	259.09	53.20
L-Oleandrosyl-oleandolide	$[M]^+$	25.758 8 ± 0.325 5^{A}	25.450 5 ± 0.361 3^{A}	22.564 7 ± 0.170 8^{B}	24.078 2 ± 0.906 8^{C}	< 0.001	530.31	500.10
L-Pipecolic acid	$[M+H]^+$	25.910 9 ± 0.248 6^{A}	25.685 0 ± 0.259 5^{A}	27.739 5 ± 0.076 6^{B}	28.450 7 ± 0.117 9^{C}	< 0.001	130.09	45.00
Maleic acid	$[M-H]^-$	23.596 1 ± 0.361 9^{A}	23.261 4 ± 1.118 5^{A}	21.865 8 ± 0.074 4^{B}	21.834 1 ± 0.039 6^{B}	< 0.05	114.99	56.60
Miglitol	$[M]^+$	20.114 9 ± 0.200 7^{A}	20.382 6 ± 0.283 7^{A}	16.783 2 ± 0.235 8^{B}	18.368 8 ± 0.464 4^{C}	< 0.001	207.11	320.10
Myriocin	$[M+H]^+$	19.122 1 ± 1.257 3^{A}	18.315 3 ± 1.161 9^{A}	21.894 3 ± 0.698 3^{B}	21.645 3 ± 1.744 0^{B}	< 0.05	402.28	366.70
N^6-Acetyl-*L*-lysine	$[M-H]^-$	25.741 6 ± 0.341 0^{A}	24.810 0 ± 0.254 8^{B}	26.868 8 ± 0.715 8^{C}	27.627 2 ± 0.375 1^{C}	< 0.001	187.11	54.30
N-Acetyl-*D*-glucosamine	$[M]^-$	23.962 7 ± 0.030 3^{A}	23.995 3 ± 0.046 9^{A}	24.427 0 ± 0.141 1^{B}	24.297 4 ± 0.092 0^{B}	< 0.001	221.16	520.20
N-Acetylornithine	$[M-H]^-$	26.276 4 ± 0.188 6^{A}	25.547 8 ± 0.197 2^{B}	23.961 5 ± 0.253 6^{C}	24.079 4 ± 0.131 6^{C}	< 0.001	173.09	55.70
N-Carbamoyl putrescine	$[M+H]^+$	24.456 3 ± 0.511 3^{A}	24.770 3 ± 0.743 1^{AB}	26.336 7 ± 0.266 4^{C}	25.573 9 ± 0.465 4^{BC}	< 0.01	132.10	571.00
Oxidized glutathione	$[M+H]^+$	20.373 7 ± 1.088 9^{A}	28.742 9 ± 0.202 2^{B}	26.603 0 ± 1.669 4^{B}	28.331 8 ± 1.123 7^{B}	< 0.001	613.15	55.10
Oxoadipic acid	$[M-H]^-$	26.167 2 ± 0.109 6^{A}	26.566 6 ± 0.008 8^{A}	25.739 5 ± 0.403 7^{B}	25.659 5 ± 0.113 8^{B}	< 0.01	158.98	130.10
Oxoglutaric acid	$[M-H]^-$	24.079 8 ± 0.019 4^{A}	24.896 3 ± 0.097 0^{B}	27.200 2 ± 0.301 9^{C}	25.985 4 ± 0.130 7^{D}	< 0.001	145.01	44.10
Phenylacetic acid	$[M]^+$	23.421 2 ± 1.035 1^{A}	24.761 3 ± 1.161 4^{A}	26.088 0 ± 0.382 0^{B}	26.174 7 ± 0.376 8^{B}	< 0.05	136.05	572.10
Prostaglandin E1	$[M+H-H_2O]^+$	21.993 1 ± 0.192 4^{A}	22.076 6 ± 0.138 8^{A}	23.074 3 ± 0.288 8^{B}	23.273 7 ± 0.419 5^{B}	< 0.001	337.23	470.00
Prostaglandin F2a	$[M+H-H_2O]^+$	22.488 6 ± 0.172 9^{A}	22.342 5 ± 0.177 1^{A}	18.964 9 ± 0.495 7^{B}	18.861 2 ± 1.883 4^{B}	< 0.01	337.24	379.40
Pyridoxine	$[M+H-H_2O]^+$	22.029 1 ± 0.082 9^{A}	22.111 3 ± 0.040 3^{A}	22.662 8 ± 0.082 1^{B}	22.357 3 ± 0.116 4^{C}	< 0.001	152.07	197.20
Pyroglutamic acid	$[M-H]^-$	23.028 9 ± 0.378 9^{A}	22.529 1 ± 0.120 7^{A}	26.228 7 ± 0.716 8^{B}	24.820 6 ± 0.352 9^{C}	< 0.001	128.04	48.40
Ribose 1,5-bisphosphate	$[M-H]^-$	27.700 7 ± 0.513 1^{A}	28.560 5 ± 0.250 0^{A}	22.519 0 ± 1.587 3^{B}	22.354 6 ± 0.481 4^{B}	< 0.001	309.17	450.20
Rosmarinic acid	$[M-H]^-$	21.932 7 ± 0.130 3^{A}	22.502 4 ± 0.148 0^{A}	18.953 5 ± 1.154 4^{B}	19.603 7 ± 0.472 2^{B}	< 0.001	359.08	241.70
Urocanic acid	$[M-H]^-$	23.616 5 ± 0.770 0^{A}	22.687 3 ± 0.826 6^{A}	21.544 9 ± 0.063 4^{B}	21.484 1 ± 0.026 1^{B}	< 0.01	137.04	60.80

Note: [a] Quantitative metabolite values were logarithmically transformed; Differential metabolites in the same altered pathways of different groups were collected and compared respectively. All data were presented in mean ± standard error. Different uppercase letters (A–D) in the same row indicated significant differences ($P < 0.05$).

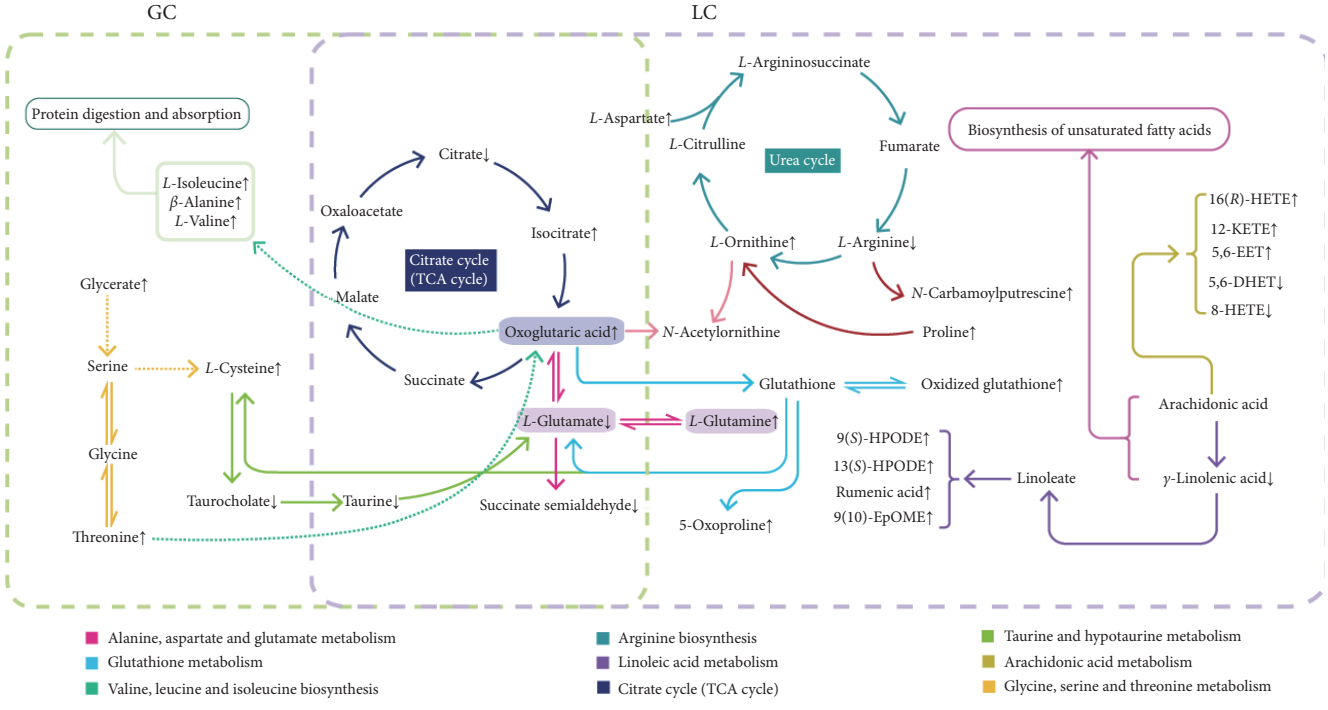

Figure 5 Linkages between metabolic pathways affected by temperature fluctuations, combining LC and GC results. The key metabolites linking the different metabolic pathways and the changes in their contents are labeled. 9(*S*)-HPODP, 9(*S*)-hydroperoxyoctadecadienoic acid; 13(*S*)-HPODE, 13(*S*)-hydroperoxyoctadecadienoic acid; 9(10)-EpOME, 9(10)-epoxy-12-octadecenoic acid.

contain most DMs. *L*-Glutamate was reduced, and its associated metabolites were raised; *γ*-linoleic acid leads to linoleate synthesis, in which degradation products are accumulated in multiple pathways (Figure S3). Arachidonic acid metabolism was more active, and the content of metabolites from arachidonic acid was altered (Figure S4). Both arachidonic acid and *γ*-linoleic acid were involved in the biosynthesis of unsaturated fatty acids, and *γ*-linoleic acid could derive from arachidonic acid.

Compared with the LC-MS, GC-MS found DMs mainly concentrated in the valine, leucine and isoleucine biosynthesis, taurine and hypotaurine metabolism, and the glycine, serine and threonine metabolism. Oxoglutaric acid can be indirectly produced from threonine and transformed into *L*-isoleucine, *β*-alanine, and *L*-valine related to protein digestion and absorption. In summary, the concentrations of protein and lipid metabolites such as *L*-valine, *L*-isoleucine, *β*-alanine, 12-KETE, and 5,6-EET in beef are significantly upregulated in the cold chain disruption. Additionally, the levels of intermediate metabolites from the TCA cycle, particularly oxoglutarate, as well as carbonyl compounds, are markedly increased. These substances can act as biomarkers indicative of beef quality degradation during cold chain interruptions, providing a basis for monitoring beef quality in cold chain logistics.

4 Discussion

The inadequacy of contemporary cold storage infrastructure, coupled with the requisite dwell times for goods in transit, are identified as the primary causes of cold chain interruption. This research investigated the effects of extended periods of cold chain interruption on the integrity of fresh beef quality and delineated the metabolites that exhibit substantial alterations in concentration throughout the course of cold chain interruptions and the metabolic pathways in which they are implicated. Furthermore, the study has succeeded in pinpointing the metabolites associated with the degradation of beef quality consequent to cold chain interruptions. These findings are instrumental in furnishing a framework for the surveillance and management of quality within beef cold chain logistics. Sensory and quality evaluation results indicated frequent temperature switches and prolonged exposure to 25 °C cause surface browning and mass duplication of microbes, collapsing the edible quality and safety (Figures 1A and F). Additionally, microbial proliferation leads to protein degradation that reduces water retention and causes more weight loss of meat in groups L2 and L3 (Figures 1D and F). Higher temperatures will severely accelerate lipid oxidation[24], which features a dominant quality assessment, leading to nutrition, flavor, texture, and appearance deterioration[25]. Moreover, group L2 was returned to 4 °C after its previous day at 25 °C. However, its TBARS value and TVB-N content kept rising obviously higher than the following day, inferring that exposure to 25 °C may trigger continuous protein and lipid oxidation, leading to irreversible deterioration in quality. Manheem et al.[26] found that meat quality change was unavoidable during cold storage. However, unstable storage temperature is a primary factor leading to more severe lipid and protein-related flavor deterioration[27], which is consistent with our study.

Additionally, the study characterized the metabolites through LC-MS and GC-MS to determine the metabolic change induced by cold chain disruption. PCA score and clustering relationship inferred that cold chain disruption reshaped the metabolic composition (Figures 2D–F, 3A and C). Notably, compared with GC-MS results, groups L2 and L3 are more similarity in the metabolic composition according to LC-MS (Figures 2D and 3A); therefore, we speculated that the later-stage cold chain interruption could trigger a quick quality collapse. Volatiles were more similar in

groups L3 and L1, which differed from group C, suggesting that flavor shift constantly occurred during storage. In the cold chain disruption groups, numerous DMs were detected and categorized into carboxylic acids and derivatives, fatty acyls, organooxygen compounds, and steroids and steroid derivatives (Figure 2A). Amino acids, peptides, and analogs were massively identified in all logistics groups as sub-metabolites classes of carboxylic acids and derivatives, indicating that protein degradation and oxidation were dominant processes in cold storage[28]. The metabolism of AA and linoleate (LA) is strengthened in cold chain disruption groups; fatty acids like 12-KETE, 16(*R*)-HETE, 5,6-EET, 9(*S*)-HPODE, and rumenic acid are metabolic products of arachidonate and LA (Figures 5 and S4), which qualified as DMs in groups L2 and L3. AA and LA are common long-chain polyunsaturated fatty acids. Linoleate dietary intake has been recognized to facilitate cardiovascular health[29]. In contrast, arachidonate metabolic processes are closely related to the development of inflammation and cardiovascular-related diseases[30]. In our results, 16(*R*)-HETE and 13(*S*)-HPODE were detected to be increased in cold chain disruption groups; *in vitro* cellular experiments demonstrated that 16(*R*)-HETE and 16(*S*)-HETE could increase the hypertrophic markers in human fetal ventricular cardiomyocytes[31], and exposure of bovine mammary endothelial cells to 13(*S*)-HPODE significantly reduced endothelial barrier integrity and increased apoptosis[32], implying that temperature changed during cold logistics will significantly up-regulated the potential health-harmful metabolites.

Notably, studies have elucidated that protein oxidation, lipid oxidation, and lipolysis in low-temperature sausage during storage were interdependent and interacted and mutually promoted each other[33], so we try to figure out the key metabolites link these process. Organooxygen compounds are the dominant class of DMs that are divided into 4 sub-classes: alcohols and polyols, carbohydrates and carbohydrate conjugates, ethers, and carbonyl compounds; in a previous study, alcohols and polyols, carbohydrates and carbohydrate conjugates were related to quality deterioration in partial freezing process of crayfish[34]. The study surmises that cold temperature disruption will cause a more severe degree of oxidation, so carbonyl compounds were assumed as a vital class of metabolites changed in cold chain disruption groups (Table S3); carbonyl compounds are produced from lipids and carbohydrates induced through non-enzymatic oxidation processes like light and heat stimulation, which can generate highly toxic unsaturated aldehydes that promotes protein oxidation and further metabolized into MDA[35–36], it binds and forms adducts with proteins to facilitates the further oxidation and function impaired[37–38]. Combined with the more acute lipid and protein oxidation within cold chain disruption and the enhancement of TBARS value (Figure 1C), the study speculated that cold chain disruption triggered the formation and consumption of carbonyl compounds to assist the collaborative oxidation processes of protein and lipid.

Finally, the most vital 9 changed metabolic pathways associated with cold chain disruption were summed up (Figure 5). The TCA cycle links amino acid and lipid metabolic processes. Its intermediate metabolites like isocitrate and oxoglutaric acid were accumulated, which is attributed to maintaining energy production to counteract adverse conditions like acute hypoxia and stress after post-slaughter[39–40]; the augmented levels of threonine and proline, implying that energy is a shortage in muscles (Figure 5, Table 1), accordingly, protein metabolism was more active under cold chain disruption, which mediated by gluconeogenesis and other pathways, are pivotal processes to product energy[41]. Metabolism of unsaturated fatty acids and the production of its secondary products may cause nutrient diminishment and toxic generation, which hurt nutritional quality and threat safety[42–43]; arachidonic acid and linoleic acid metabolism were more dynamic in cold chain disruption groups, γ-linoleic acid can be produced from arachidonic acid and further generate linoleate that communicates arachidonic acid and linoleic acid metabolic process.

In summary, the study discussed the impact of 3 different cold chain disruption sceneries on the quality of beef and identified pivotal metabolites that correlate with the degradation of beef quality during the process of cold chain disruption, and the quality deterioration were acute with the increase of interrupts number. Physicochemical properties shows that cold chain interruption exacerbated the quality deterioration. Metabolomics results show that carbonyl compounds are dominant DMs that engage in flavor degradation and induce varied nutrients' synergistic oxidation, which may be triggered by higher storage temperature. In the end, the metabolic net suggests a strong link between the energy-producing related TCA cycle and the protein degradation pathway, suggesting that energy is scarce in post-slaughter beef and protein catabolism is reinforced to generate energy. However, this study did not extensively focus on the impact of temperature and time and their interaction on meat quality in the cold chain interruption. The effects of temperature and the duration of cold chain disruption on meat quality and metabolism are worthy of deep investigation.

5 Conclusion

Cold chain disruptions significantly deteriorate the sensory qualities of fresh beef and activate lipid and protein degradation, resulting in elevated levels of lipid and protein metabolites, including *L*-valine, *L*-isoleucine, β-alanine, 12-KETE, and 5,6-EET. Moreover, there is a marked increase in oxoglutaric acid, a crucial intermediate in the TCA cycle, which links protein degradation processes and post-slaughter energy production. Additionally, the levels of carbonyl compounds exhibit a notable upregulation, which is closely associated with the oxidation of proteins and lipids. In this study, we elucidate the metabolic changes and quality deterioration in fresh beef caused by cold chain interruptions, offering a novel perspective for monitoring beef quality in cold chain circulation.

Author contributions

Zhanfei Deng: Investigation; formal analysis; writing (original draft, review and editing); visualization; software. **Shuangshuang Sun**: Methodology; investigation. **Yuyue Shi**: Methodology; investigation. **Yayun Hu**: Methodology; investigation. **Xin Lü**: Supervision; resources. **Yuanyuan Shan**: Supervision; conceptualization; investigation; project administration.

Declaration of competing interest

The authors declare no conflict of interest.

Acknowledgments

The authors gratefully acknowledge the financial support from the Science and Technology Major Project of Xinjiang Uygur Autonomous Regions (2022A02006-4). We would also like to thank the instrument-sharing platform of NWAFU for the assistance in the Texture Analyzer and technical support.

References

[1] H. H. H. Mohammed, L. C. He, A. Nawaz, et al., Effect of frozen and refrozen storage of beef and chicken meats on inoculated microorganisms and meat quality, Meat Sci. 175 (2021) 108453. https://doi.org/10.1016/j.meatsci.2021.108453.

[2] I. A. Chiurciu, E. Soare, P. Stoicea, et al., Research on the evolution of the global beef market in the period 2015–2020, Scientific Papers 22(4) (2022) 169–176.

[3] S. L. Deng, Y. Q. Han, T. X. Gao, et al., Effect of temperature fluctuation during frozen storage on beef quality, J. Food Process. Preserv. 45 (2021) e15043. https://doi.org/10.1111/jfpp.15043.

[4] Y. J. Qiu, Y. Zhou, Y. F. Chang, et al., The effects of ventilation, humidity, and temperature on bacterial growth and bacterial genera distribution, Int. J. Environ. Res. Public. Health 19 (2022) 15345. https://doi.org/10.3390/ijerph192215345.

[5] S. P. Yang, J. Xie, Z. L. Gao, et al., Effect of temperature and time fluctuations on quality changes of iced *Trichiurus haumela* in cold chain logistics process, Trans. Chin. Soc. Agric. Eng. 29 (2013) 302–310. https://doi.org/10.3969/j.issn.1002-6819.2013.24.039.

[6] S. Mercier, S. Villeneuve, M. Mondor, et al., Time-temperature management along the food cold chain: a review of recent developments, Compr. Rev. Food Sci. Food Saf. 16 (2017) 647–667. https://doi.org/10.1111/1541-4337.12269.

[7] Q. S. Ren, K. Fang, X. T. Yang, et al., Ensuring the quality of meat in cold chain logistics: a comprehensive review, Trends Food Sci. Technol. 119 (2022) 133–151. https://doi.org/10.1016/j.tifs.2021.12.006.

[8] G. Lorentzen, T. N. Ageeva, M. Heide, et al., Temperature fluctuations in processing and distribution: effect on the shelf life of fresh cod fillets (*Gadus morhua* L.), Food Control 112 (2020) 107102. https://doi.org/10.1016/j.foodcont.2020.107102.

[9] Y. R. Tang, J. Xie, N. W. Li, et al., Effects of different cold chain logistics processes on the quality and histomorphology of tuna fish, J. Agric. Eng. 30 (2014) 285–292. https://doi.org/10.3969/j.issn.1002-6819.2014.05.036.

[10] Y. J. Yu, S. P. Yang, T. Lin, et al., Effect of cold chain logistic interruptions on lipid oxidation and volatile organic compounds of salmon (*Salmo salar*) and their correlations with water dynamics, Front. Nutr. 7 (2020) 155. https://doi.org/10.3389/fnut.2020.00155.

[11] K. Y. Wang, T. L. Yip, Cold-chain systems in china and value-chain analysis, in: S. Gong, K. Cullinane (Eds.), Finance and risk management for international logistics and the supply chain, Elsevier, 2018, pp. 217–241. https://doi.org/10.1016/B978-0-12-813830-4.00009-5.

[12] H. Luo, M. J. Zhu, S. G. Ye, et al., An intelligent tracking system based on internet of things for the cold chain, Int. Res. 26 (2016) 435–445. https://doi.org/10.1108/IntR-11-2014-0294.

[13] W. X. Zhang, L. Pan, L. X. Lu, Prediction of TVB-N content in beef with packaging films using visible-near infrared hyperspectral imaging, Food Control 147 (2023) 109562. https://doi.org/10.1016/j.foodcont.2022.109562.

[14] R. Balti, M. Ben Mansour, N. Zayoud, et al., Active exopolysaccharides based edible coatings enriched with red seaweed (*Gracilaria gracilis*) extract to improve shrimp preservation during refrigerated storage, Food Biosci. 34 (2020) 100522. https://doi.org/10.1016/j.fbio.2019.100522.

[15] H. X. Lin, S. S. Zhao, X. Y. Han, et al., Effect of static magnetic field extended supercooling preservation on beef quality, Food Chem. 370 (2022) 131264. https://doi.org/10.1016/j.foodchem.2021.131264.

[16] L. H. Ge, Y. S. Xu, W. S. Xia, et al., Differential role of endogenous cathepsin and microorganism in texture softening of ice-stored grass carp (*Ctenopharyngodon idella*) fillets, J. Sci. Food Agric. 96 (2016) 3233–3239. https://doi.org/10.1002/jsfa.7506.

[17] C. Y. Liu, C. T. Fu, J. R. Xu, et al., Study on the quality change of buffalo meat during low-temperature storage, Sci. Technol. Food Ind. 41 (2020) 273–278; 287. https://doi.org/10.13386/j.issn1002-0306.2020.02.043.

[18] M. Navarro-Reig, J. Jaumot, A. García-Reiriz, et al., Evaluation of changes induced in rice metabolome by Cd and Cu exposure using LC-MS with XCMS and MCR-ALS data analysis strategies, Anal. Bioanal. Chem. 407 (2015) 8835–8847. https://doi.org/10.1007/s00216-015-9042-2.

[19] D. S. Wishart, D. Tzur, C. Knox, et al., HMDB: the Human Metabolome Database, Nucleic Acids Res. 35 (2007) D521–D526. https://doi.org/10.1093/nar/gkl923.

[20] H. Ogata, S. Goto, K. Sato, et al., KEGG: Kyoto Encyclopedia of Genes and Genomes, Nucleic Acids Res. 27 (1999) 29–34. https://doi.org/10.1093/nar/28.1.27.

[21] M. Sud, E. Fahy, D. Cotter, et al., LMSD: LIPID MAPS structure database, Nucleic Acids Res. 35 (2007) D527–D532. https://doi.org/10.1093/nar/gkl838.

[22] J. Xia, D. S. Wishart, Web-based inference of biological patterns, functions and pathways from metabolomic data using MetaboAnalyst, Nat. Protoc. 6 (2011) 743–760. https://doi.org/10.1038/nprot.2011.319.

[23] Y. B. Zhou, Q. J. Ai, D. Q. Zhang, Analysis of microbial flora changes on the surface of cold fresh mutton during 4 °C storage period, Food Sci. 36 (2015) 242–245. https://doi.org/10.7506/spkx1002-6630-201506046.

[24] Q. Xiong, M. H. Zhang, T. Wang, et al., Lipid oxidation induced by heating in chicken meat and the relationship with oxidants and antioxidant enzymes activities, Poult. Sci. 99 (2020) 1761–1767. https://doi.org/10.1016/j.psj.2019.11.013.

[25] D. Wang, H. Xiao, X. Lyu, et al., Lipid oxidation in food science and nutritional health: a comprehensive review, Oil Crop Sci. 8 (2023) 35–44. https://doi.org/10.1016/j.ocsci.2023.02.002.

[26] K. Manheem, O. Adiamo, U. Roobab, et al., A comparative study on changes in protein, lipid and meat-quality attributes of camel meat, beef and sheep meat (mutton) during refrigerated storage, Animals 13 (2023) 904. https://doi.org/10.3390/ani13050904.

[27] Y. Tao, Y. P. Guo, J. W. Li, et al., Effect of temperature fluctuation during superchilling storage on the microstructure and quality of raw pork, Meat Sci. 198 (2023) 109096. https://doi.org/10.1016/j.meatsci.2023.109096.

[28] H. J. Han, M. H. Li, Y. M. Liu, et al., Non-volatile metabolite changes in low-temperature sausage stored at room temperature, Food Packag. Shelf Life 31 (2022) 100805. https://doi.org/10.1016/j.fpsl.2021.100805.

[29] F. Marangoni, C. Agostoni, C. Borghi, et al., Dietary linoleic acid and human health: focus on cardiovascular and cardiometabolic effects, Atherosclerosis 292 (2020) 90–98. https://doi.org/10.1016/j.atherosclerosis.2019.11.018.

[30] Y. R. Zhang, Y. X. Liu, J. Sun, et al., Arachidonic acid metabolism in health and disease, MedComm 4 (2023) e363. https://doi.org/10.1002/mco2.363.

[31] R. Hidayat, M. A. El-Ghiaty, S. M. Shoieb, et al., The effects of 16-HETE enantiomers on hypertrophic markers in human fetal

ventricular cardiomyocytes, RL-14 Cells, Eur. J. Drug Metab. Pharmacokinet. 48 (2023) 709–722. https://doi.org/10.1007/s13318-023-00857-1.

[32] V. E. Ryman, N. Packiriswamy, L. M. Sordillo, Apoptosis of endothelial cells by 13-HPODE contributes to impairment of endothelial barrier integrity, Mediators Inflamm. 2016 (2016) 1–13. https://doi.org/10.1155/2016/9867138.

[33] H. J. Han, Z. H. Zhang, J. N. Wang, et al., Elucidating the cause of variation in low-temperature sausage protein oxidation along storage period via lipid oxidation and lipolysis, J. Food Process. Preserv. 46 (2022) e16708. https://doi.org/10.1111/jfpp.16708.

[34] X. L. Huang, Z. C. Tu, W. Y. Liu, et al., Effect of three culture patterns on quality changes of crayfish meats during partial freezing storage, Food Chem. 414 (2023) 135683. https://doi.org/10.1016/j.foodchem.2023.135683.

[35] Q. Huang, K. Dong, Q. Wang, et al., Changes in volatile flavor of yak meat during oxidation based on multi-omics, Food Chem. 371 (2022) 131103. https://doi.org/10.1016/j.foodchem.2021.131103.

[36] N . Liu, K. X. Cui, Y. Sun, Research progress of active carbonyl compounds produced by oxidantion of fats in food, Sci. Technol. Food Ind. 43 (17) (2022) 466–473. https://doi.org/10.13386/j.issn1002-0306.2021090098.

[37] M. Breitzig, C. Bhimineni, R. Lockey, et al., 4-Hydroxy-2-nonenal: a critical target in oxidative stress?, Am. J. Physiol. Cell Physiol. 311 (2016) C537–C543. https://doi.org/10.1152/ajpcell.00101.2016.

[38] I. M. Møller, A. Rogowska-Wrzesinska, R. S. P. Rao, Protein carbonylation and metal-catalyzed protein oxidation in a cellular perspective, J. Proteomics 74 (2011) 2228–2242. https://doi.org/10.1016/j.jprot.2011.05.004.

[39] R. Wang, Y. Guo, Z. Shi, et al., A quantitative proteomic analyses of primary myocardial cell injury induced by heat stress in chicken embryo, J. Therm. Biol. 112 (2023) 103461. https://doi.org/10.1016/j.jtherbio.2023.103461.

[40] L. L. Zhao, L. Liao, H. X. Yan, et al., Physiological responses to acute hypoxia in the liver of largemouth bass by alteration of mitochondrial function and Ca^{2+} exchange, Aquat. Toxicol. 256 (2023) 106436. https://doi.org/10.1016/j.aquatox.2023.106436.

[41] M. Ijaz, D. Zhang, C. Hou, et al., Changes in postmortem metabolites profile of atypical and typical DFD beef, Meat Sci. 193 (2022) 108922. https://doi.org/10.1016/j.meatsci.2022.108922.

[42] N. Hematyar, T. Rustad, S. Sampels, et al., Relationship between lipid and protein oxidation in fish, Aquac. Res. 50 (2019) 1393–1403. https://doi.org/10.1111/are.14012.

[43] N. Tenyang, B. Tiencheu, F. Tonfack Djikeng, et al., Alteration of the lipid of red carp (*Cyprinus carpio*) during frozen storage, Food Sci. Nutr. 7 (2019) 1371–1378. https://doi.org/10.1002/fsn3.971.